W. Szemplińska-Stupnicka
J. Rudowski

STEADY STATES IN THE TWIN-WELL
POTENTIAL OSCILLATOR:
COMPUTER SIMULATIONS AND
APPROXIMATE ANALYTICAL STUDIES

40/1992

P.269

WARSZAWA 1992

Praca wpłynęła do Redakcji dnia 25 września 1992 r.

N a   p r a w a c h   r ę k o p i s u

Wanda Szemplińska-Stupnicka
Jerzy Rudowski
Samodzielna Pracownia Dynamiki Stosowanej

STEADY STATES IN THE TWIN-WELL POTENTIAL OSCILLATOR:

COMPUTER SIMULATIONS AND APPROXIMATE ANALYTICAL STUDIES

ABSTRACT

The paper is focused on the phenomena of various steady state oscillations exhibited by the twin-well potential system. Regions of existence of different attractors in the system parameter domain are examined and a picture book of different steady states for fixed damping and forcing is presented: 20 different combinations of single or coexisting, Small Orbit or Large Orbit, periodic and chaotic attractors are displayed.

Computer simulations are followed by an approximate analytical analysis: a study of various forms of instability of periodic solutions gives close form approximate criteria for occurrence of T-periodic Small Orbit and Large Orbit oscillations, and for cross-well chaos.

## 1. INTRODUCTION

The sinusoidally driven twin-well oscillator governed by equation in the form:

$$(1) \qquad \ddot{x} + h\dot{x} - \bar{\alpha}x + \beta\bar{x}^3 = F \cos \omega t ,$$

$$h > 0 , \quad \alpha > 0 , \quad \beta > 0 , \qquad T = \frac{2\Pi}{\omega}$$

has become a classic central model for analysis of inherently

nonlinear phenomena, the phenomena in which enormously complex chaotic motion and highly regular periodic behavior can coexist or to neighbor upon each other in the system parameter domain.

The equation was originally studied by Holmes and Moon since 1979 and was derived as mathematical model of a buckled beam or of plasma oscillations (Mahaffey [1],Moon [2], Moon and Li [3]).

The simplest experimental device for eqs(1) is that depicted in Fig. 1: a particle placed in a twin-well potential with the base vibrating with periodic motion. When the amplitude of excitation is large enough the particle escapes from one of the potential well and can jump from one well to the other in random-like, irregular manner.
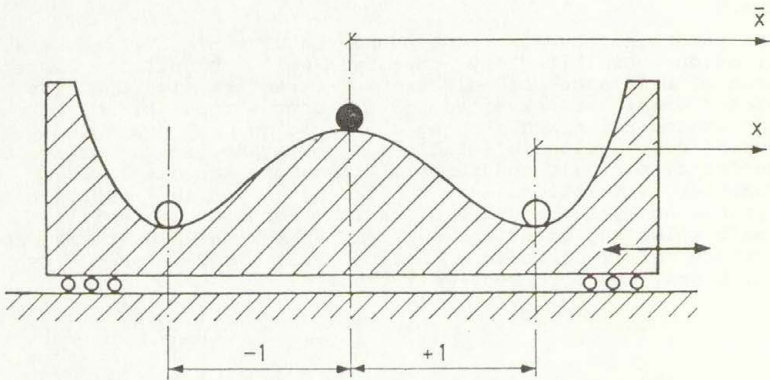


Fig. 1. A physical model of twin-well potential oscillator.

The equation is also a classic model for the study of various complex bifurcation phenomena, fractal basins boundaries between competing coexisting attractors and the related problem of sensitivity to initial conditions, homoclinic tangling of the invariant manifolds of saddle point and the Melnikov criterion, fractal dimensions of strange attractors and Lapunov exponents

(Arecci and Califano [4], Grebogi, Ott and Yorke [5],Guckenheimer and Holmes [6], Holmes [7], Holmes and Moon [8], McDonald, Grebogi, Ott and Yorke [9], Moon and Li [3,10], Pezeshki and Dowell [11,12], Szemplińska, Joos and Moon [13], Szemplińska [14], Szemplińska, Plaut and Hsieh [15], Tang and Dowell [16], Ueda, Yoshida, Stewart and Thompson [17]). The problem of criteria for chaos received also a great deal of attention and was examined by numerical, experimental and analytical methods (Moon [2], Guckenheimer and Holmes [6], Dowell and Pezeshki[18], Dowell [19], Szemplińska [14,20], Szemplińska, Plaut and Hsieh [15], Szemplińska and Rudowski [21]). Some attempts toward constructing the analytical approximate criteria is also due to Moon [22], Takimoto and Yamashida [23], Virgin [24].

The aim of this paper is two-fold: first we want to present a picture book of various, unique or coexisting steady states exhibited in the system (1) at fixed damping and within the range driving frequency, which covers the principal and 2-nd order superharmonic resonance, $0.25 \leq \omega \leq 1.1$. Second, we show that the approximate theory of nonlinear oscillations, and in particular, stability analysis of an approximate periodic solution, makes it possible to estimate the system parameter domains, where certain types of steady state occur, and to predict boundaries of the region, where the system exhibits cross-well chaotic motion. The approximate study involves the T-periodic second approximate solution of eqs. (1) obtained by a perturbation method, and the analysis of various forms of instability of the solution by considering approximate solutions of Hill's type variational equation. This enables us to calculate domains of existence of stable symmetric T-periodic Large Orbit solution (trajectory, which encircles all equilibria) and the domain, where the T-periodic Small Orbit attractor does not exist. The latter provides us with the approximate criterion for the system parameters critical values, for which the system exhibits cross-well chaotic motion.

Good coincidence of computer simulations and the approximate

theoretical results throws new light on some traditional concepts and views: the results seem to blur the distinction between weak and strong nonlinearity, and to explain why the apparently close neighborhood of regular nearly harmonic response and the complex, continuous spectrum chaotic solution, makes the approximate methods applicable in detecting strange phenomena domains. The results help us also to find out a close relationship between the classic nonlinear phenomena, such as principal, super- or subharmonic resonances and the bifurcations, which lead to the strict loss of stability of a periodic attractor and to the escape from a potential well.

## 2.. STEADY STATES IN THE NEIGHBORHOOD OF PRINCIPAL AND SUPERHARMONIC RESONANCE.

First we notice, that the three equilibrium positions of the system (1) are defined by:

(2a)    $-\alpha x + \beta x^3 = 0$ ,

$$x^{(s)}_{1,2} = \mp\sqrt{\frac{\alpha}{\beta}}\ ,\qquad \text{- stable equilibria}$$

$$x^{(s)}_{3} = 0 \qquad\qquad \text{unstable equilibria (saddle point)}$$

and that the oscillations around the stable rest point are governed by equation:

(2b)    $\ddot{x} + h\dot{x} + 2\alpha x \mp 3\sqrt{\alpha\beta}\ x^2 + \beta x^3 = F\cos\omega t$ ,

where

$$x = \bar{x} \mp \sqrt{\frac{\alpha}{\beta}}\ .$$

Setting $\alpha = \beta = \frac{1}{2}$ gives us a normalized system, in which the linear natural frequency and the positions of stable equilibria are given as:

$$\Omega_0^2 = 2\alpha = 1 \ ,$$

$$x_{1,2}^{(s)} = \mp 1 \ ;$$

Therefore we consider the system (1) reduced to the form:

(3) $$\ddot{x} + h\dot{x} - \frac{1}{2}\bar{x} + \frac{1}{2}\bar{x}^3 = F \cos \omega t \ ,$$

and that for the deflection from the stable rest point, eqs. (2b) as:

(4) $$\ddot{x} + h\dot{x} + x \mp \frac{3}{2}x^2 + \frac{1}{2}x^3 = F \cos \omega t \ ;$$

From the theory of nonlinear oscillations we have learned that the system can exhibit two types of periodic motion: Small Orbit i.e. oscillations around one of the two stable equilibria and Large Orbit motion, i.e. large amplitude oscillations which encircle all three rest points (Fig. 2).
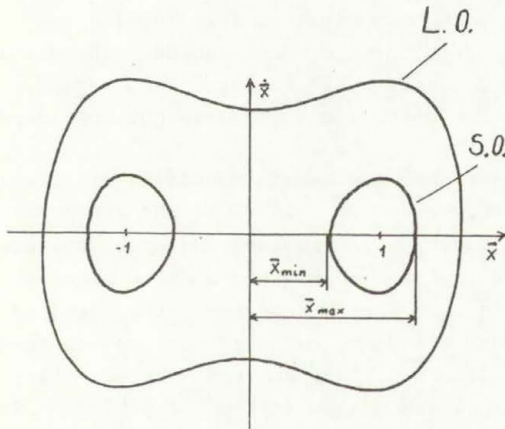


Fig. 2. Two types of periodic motion: S.O. - Small Orbit, L.O. - Large Orbit.

Equation (4), for the Small Orbit motion, is a classic, dissipative, driven oscillator with quadratic and qubic nonlinearity. When we observe the Small Orbit motion in the neighborhood of the principal resonance, i.e. at $\omega \approx 1$, we notice that the resonance curve $x_{max} \equiv x_{max}(\omega)$ is bent to the left, i.e. that it has softening restoring force characteristic. At sufficiently low values of the forcing term F the response is close to a harmonic function of time, with the driving frequency $\omega$, and it shows classic jump phenomena and hysteresis behavior (see Fig. 3a). When F exceeds certain critical value denoted as $F_1$, $F_1 < F < F_2$, the T-periodic nearly harmonic response bifurcates into 2T-periodic solution at the top of the resonant branch of the resonance curve, but still "jumps" down to the nonresonant branch and the hysteresis behavior still occurs (Fig. 3b). On further increase of the parameter F, $F > F_2$, the classic Feigenbaum Period Doubling cascade (Feigenbaum [25]) occurs and the system escapes from the potential well x = 0 and falls into the other well. Because properties of the two Small Orbits are identical (one is the mirror image of the other) the cross-well chaotic motion develops (Fig. 3c).
Sometimes Small Orbit chaos can be also detected within a very narrow frequency band, just before the escape, but the phenomenon seems to be negligible and is not considered in this paper.

Therefore the higher frequency boundary of the cross-well chaos, the boundary which is related to the resonant branch of the resonance curve, is preceded by the universal period doubling cascade, All the enormously complex bifurcations occur, however, within a very narrow frequency zone, denoted as $\Delta\omega$ in Fig. 3c. The lower frequency boundary corresponds to saddle-node bifurcation (cyclic fold, Thompson and Stewart [26], Thompson [27,28]). Here a sudden change to/from T-periodic Small Orbit from/to chaotic attractor occurs and the two different steady states are separated by transient motion only. This is often referred to as crisis phenomena, or crisis type transition
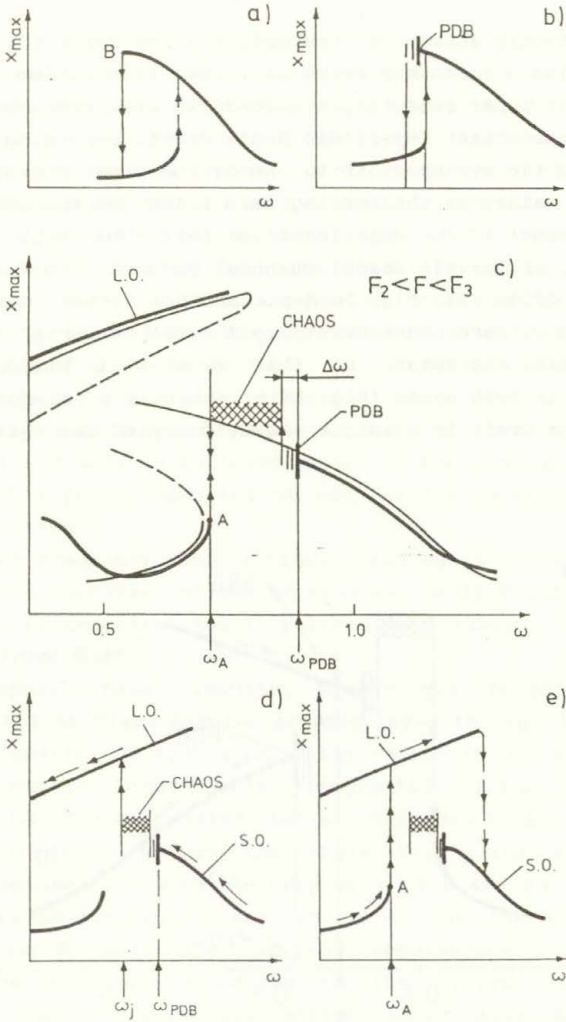
Fig. 3. Resonance curves and bifurcation in the principal resonance region: (a) Small Orbit, $F < F_1$. (b) Small Orbit, $F_1 < F < F_2$. (c) $F_2 < F < F_3$ - Small Orbit and coexisting Large Orbit motion. (d,e) Interaction of Small and Large Orbit motion, $F > F$ .

to/from chaotic attractor (Grebogi, Ott and Yorke [5]). Fig. 3c
depicts also a resonance curve of Large Orbit motion. Here the
Large Orbit T-periodic response coexists with cross-well chaos,
or with nonresonant T-periodic Small Orbit. Depending on initial
conditions the system exhibits one or the other steady state.

Higher values of the forcing term brings an appearance of a
new phenomena: if the experiment is performed with decreasing
frequency, cross-well chaos changes suddenly to Large Orbit
Attractor (Fig. 3d). Fig. 3e depicts the system behavior for
decreasing ω: here nonresonant Small Orbit response jumps into
Large Orbit attractor, so that cross-well motion is not
observed. In both cases (Fig. 3d-e) there is a frequency zone,
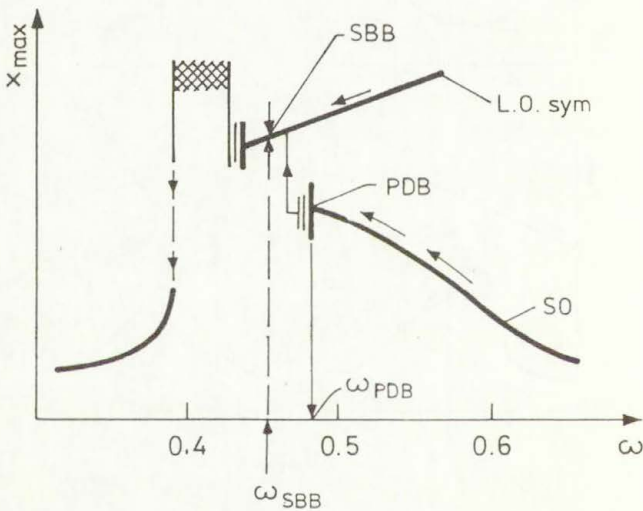where Large Orbit is a unique steady state of the system.



Fig. 4. Resonace curves, bifurcation and interaction of L.O.
and S.O. at the superharmonic resonance region.

Next Fig. 4 depicts the mechanism of transition to steady state cross-well chaos, which occurs in the neighborhood of the 2-nd order superharmonic resonance, i.e. close to $\omega = 0.5$. Here both types of regular responses - Small and Large Orbit lose their stability and disappear of a sequence of complex bifurcations, giving rise to unique chaotic attractor. If the numerical experiment begins at $\omega > 0.5$ with the initial conditions, which generate Small Orbit motion, and is performed on decreasing $\omega$, the classic period doubling cascade is observed. Yet, instead of changing into cross-well chaos, the response "jumps" up to Large Orbit. On further decrease of the driving frequency T-periodic symmetric Large Orbit attractor bifurcates into an unsymmetric one (a pair of two unsymmetric attractors) and this is followed again by the cascade of period doublings. This period doubling cascade results in transition to cross-well chaos.

The lower frequency band of chaotic region is related to the saddle-node bifurcation of the nonresonant Small Orbit solution (cycle fold bifurcation) and is related to a sudden, crisis type change to/from chaotic attractor.

The computer based results, within the frequency zone $0.25 < \omega < 1.1$ at fixed damping are displayed in Fig. 5-8.

Fig. 5 depicts the system parameter region $(F,\omega)$, where Small Orbit, symmetric Large Orbit, unsymmetric Large Orbit and cross-well chaotic or regular stable attractors exist. The Small Orbit motion occurs within the whole F-$\omega$ plane except two V-shaped regions: one with the cusp at $\omega \approx 0.8$ and $F = F_2$ at the principal resonance region (see Fig. 3a-e), and the other cusp at $\omega \approx 0.4$ and $F \approx 0.14$ i.e. at the superharmonic resonance zone. Inside the two V-shaped regions the system can exhibit cross-well chaotic (or regular) motion. We see also that in some regions two different attractors coexist, while in the others single steady state motion can be observed. In the latter case we can say, that the attractors are globally stable. In the case of two coexisting steady states we deal with the question of their domains of attractions, but the problem is not studied in
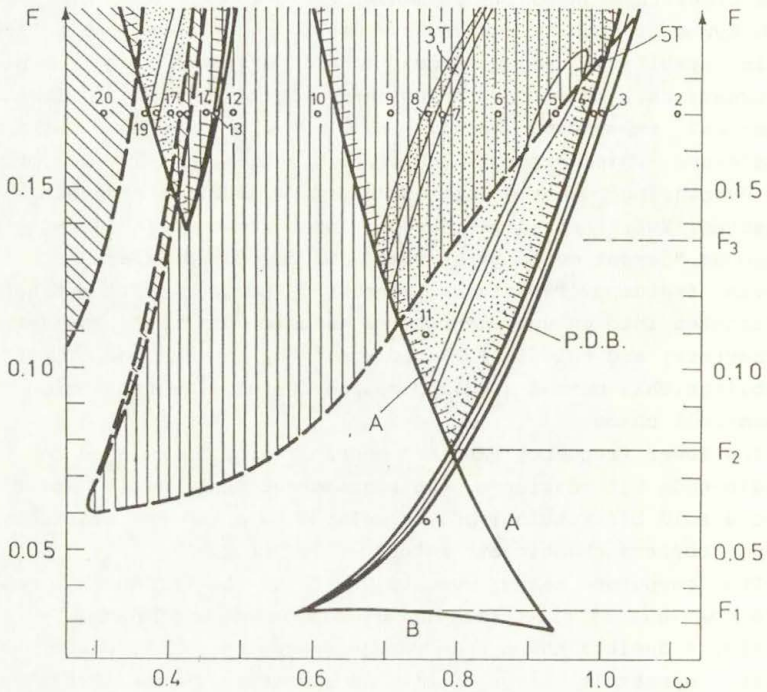
this paper.



Fig. 5. Regions of different steady states exhibited by the twin-well potential oscillator. h = 0.1.

|||||||||| L.O. symmetric,   \\\\\\\ L.O. unsymmetric,

░░░░░░ cross-well chaotic motion,

S.O. occur outside V-shaped regions.

The various single and coexisting steady states denoted in Fig. 5 as 1 , 2 ... 20 are then shown in Fig. 6: regular attractors are illustrated by their phase-portraits and chaotic attractors - by Poincare maps.
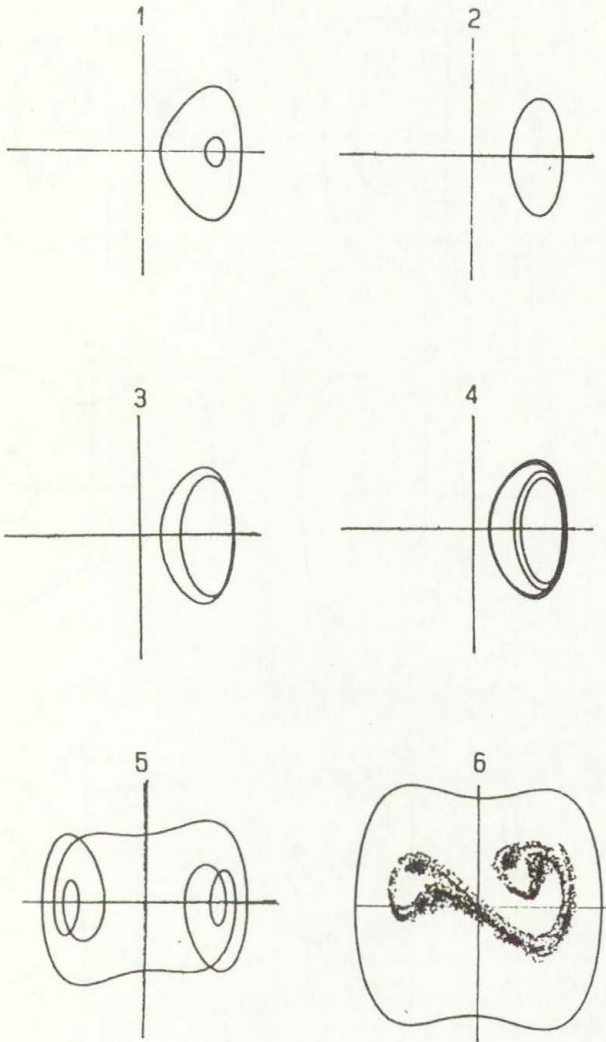
Fig. 6. Various types of steady state attractors: h = 0.1

① F = 0.06, ω = 0.74; F = 0.17: ② ω = 1.1;

③ ω = 1.0; ④ ω = 0.982; ⑤ ω = 0.93; ⑥ ω - 0.85.
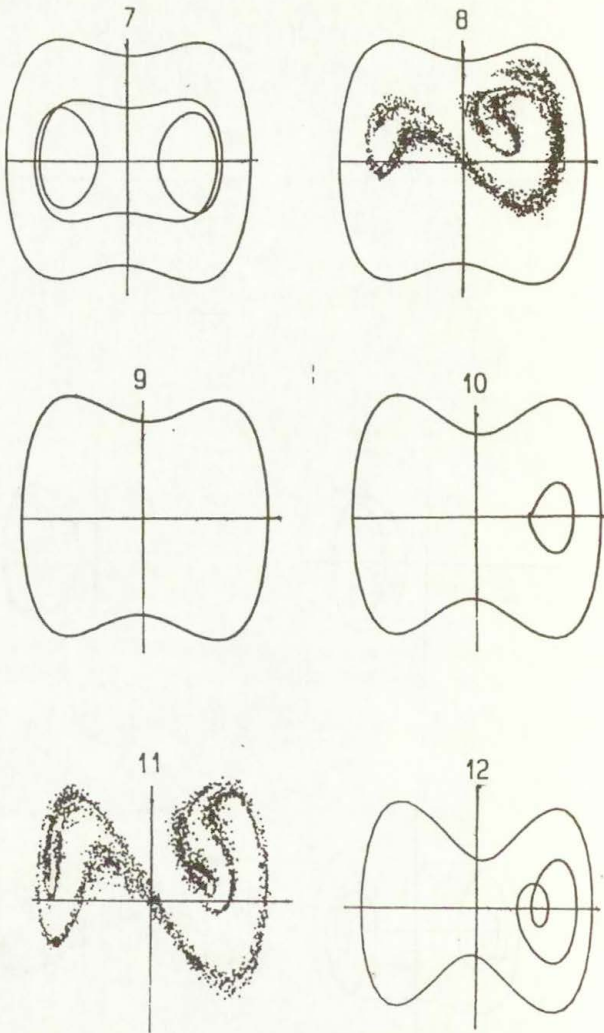
Fig. 6 continued: F =0.17: ⑦ ω = 0.79; ⑧ ω = 0.75;
⑨ ω = 0.70; ⑩ ω = 0.60; ⑪ F = 0.11, ω = 0.75;
⑫ F = 0.17, ω = 0.48.
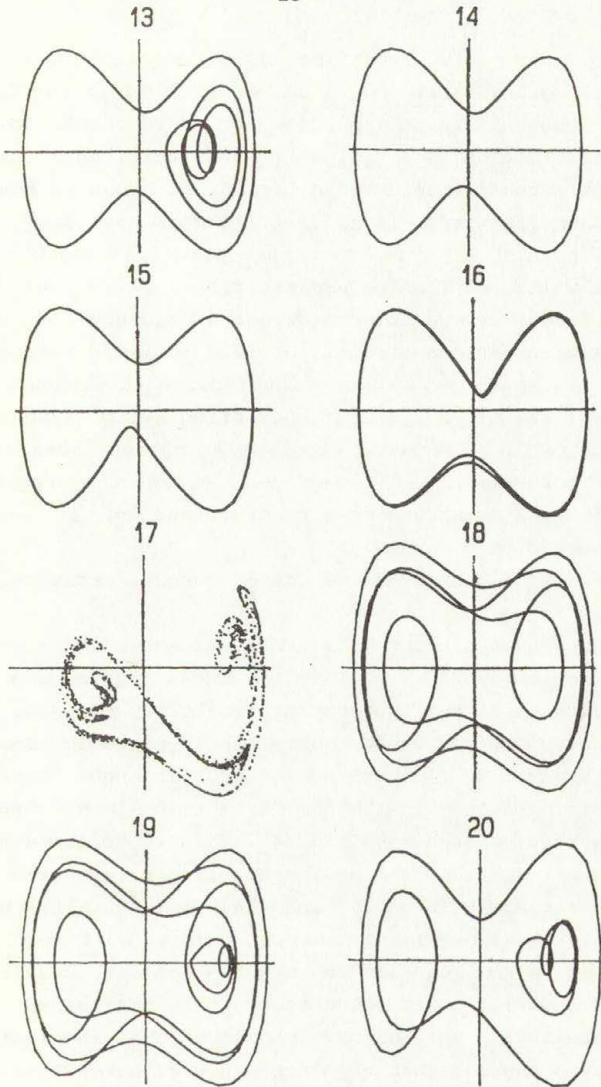
Fig. 6 continued: F =0.17: (13) ω = 0.45; (14) ω = 0.44;
(15) ω = 0.41; (16) ω = 0.4045; (17) ω = 0.40;
(18) ω = 0.3845; (19) ω = 0.38; (20) ω = 0.30.

First point 1 shows periodic response close to the principal resonance at low values of F ($F < F_2$): the system can exhibit resonant, large amplitude, or nonresonant, low amplitude Small Orbit motion (see Fig. 3b). Note that only Right Small Orbit attractor is depicted in Fig. 6, although we realize, that the Left one, a mirror image of it, always coexists.

Then, points 2 - 10 cover the principal resonance region at large values of forcing parameter $F = 0.17 > F_3$, at decreasing driving frequency. We observe here the sequence of two period doubling bifurcations of Small Orbit T-periodic response (points 2 - 4), cross-well periodic motion ("periodic window") - p. 5, cross-well chaotic attractor coexisting with symmetric Large Orbit (p. 6), 3T periodic cross-well motion coexisting with L.O. attractors (p. 8). Point 9 lies in the region, where symmetric L.O. is an unique attractor, and p. 10 show again coexistence of L.O. and S.O.

Point 11 illustrates the case, where cross-well chaotic motion is an unique attractor.

The consequtive points 12 - 20 cover the zone of the superharmonic resonance. Point 12 shows again the L.O. and S.O. coexistence, but the complex trajectory of S.O. indicates multi-frequency response. Next the T-periodic Small Orbit bifurcates into 2T (further period doubling not detected) and disappears, leaving us with the symmetric Large Orbit as an unique attractor (see also Fig. 4). This is followed by Symmetry Breaking bifurcation, and period doubling bifurcation of Large Orbit attractor (points 15 and 16) and finally by chaotic (point 17) and regular (point 18) cross well motion. Point 19 shows also regular cross-well motion. coexisting with T-periodic Small Orbit attractor, the phenomena, which was detected within a very narrow frequency zone. The last point 20 illustrates the superharmonic resonance of Large Orbit solution: this is strongly unsymmetric Large Orbit T-periodic motion, in which constant term and second harmonic are of the same order as the fundamental harmonic.

Fig. 7a-g give more details about some of the steady-state

motions: from Fig. 7a, we learn that the T-periodic Small Orbit at p. 2 involves large fundamental harmonic, and small second harmonic and constant term; Fig. 7b tells us, that the first period doubling bifurcation manifests itself by an appearance of harmonic component with frequency $\frac{1}{2}\omega$ and $\frac{3}{2}\omega$.

Fig. 7c depicts cross-well chaos characteristics at $\omega = 0.97$, i.e. very close to the boundary of chaotic region. In this strange attractor the difference in image density is observed (Ueda [29,30]).

Next Figs. 7d,e show time histories, phase portraits, frequency spectrum and Poincare map of the two "periodic window" attractors (points 5 and 7). The four characteristics of cross-well chaotic attractor in point 6 are depicted in Fig. 7f.

Results presented in Fig. 7g lead to surprising conclusions: the large amplitude Large Orbit appears to be highly regular and very close to harmonic function of time, with frequency $\omega$.

Fig. 8a,b are aimed to illustrate the phenomenon of 2-nd order superharmonic resonance of Large Orbit solution: the response is strongly unsymmetric, the constant term and second harmonic component are of the same order as the fundamental frequency component. Fig. 8b shows the corresponding resonance curves and illustrates the loss of stability of the solution at $\omega \approx 0.325$, thus explaining the disappearance of the unsymmetric Large Orbit at higher values of the driving frequency (see Fig. 5).

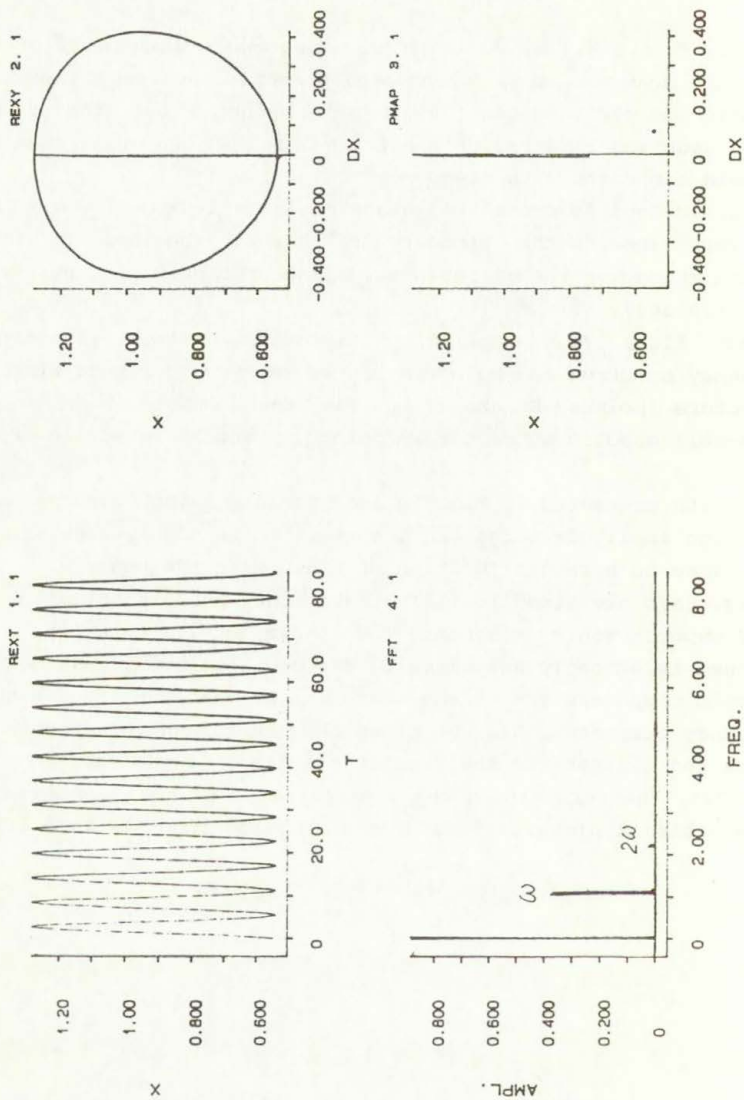Fig. 7. Time histories, phase portraits, Fourier spectra and
Poincare maps of various steady state motions: F = 0.17,
h = 0.1; (a) - ω = 1.1.

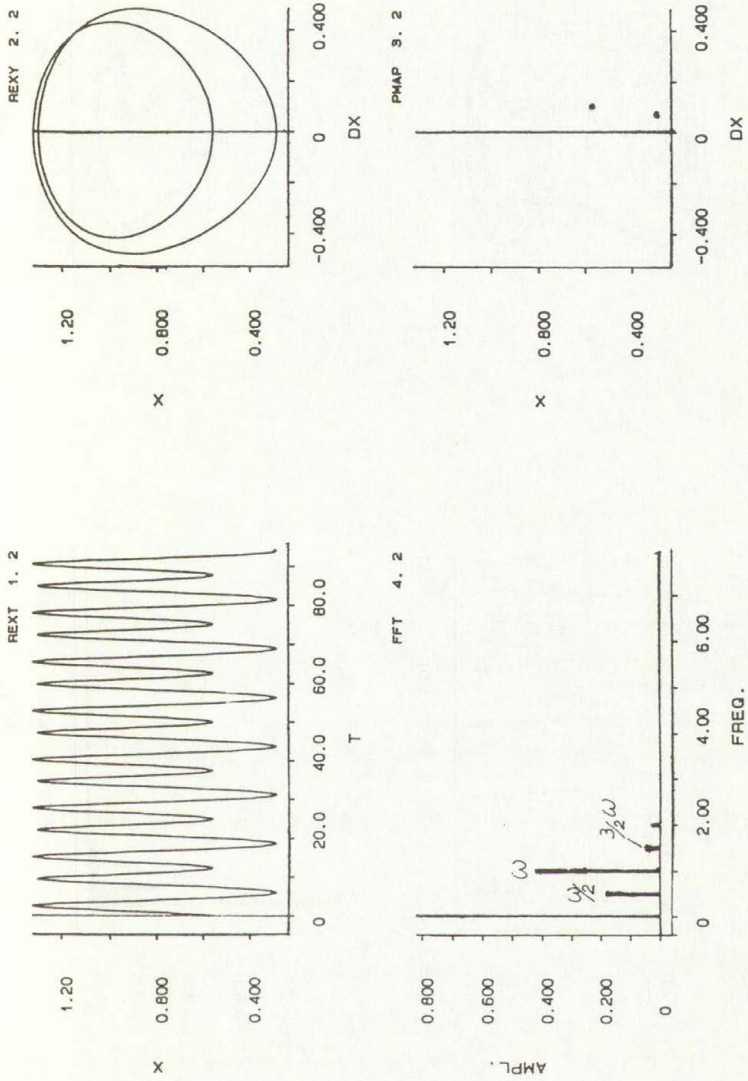Fig. 7b. $\omega = 1$.

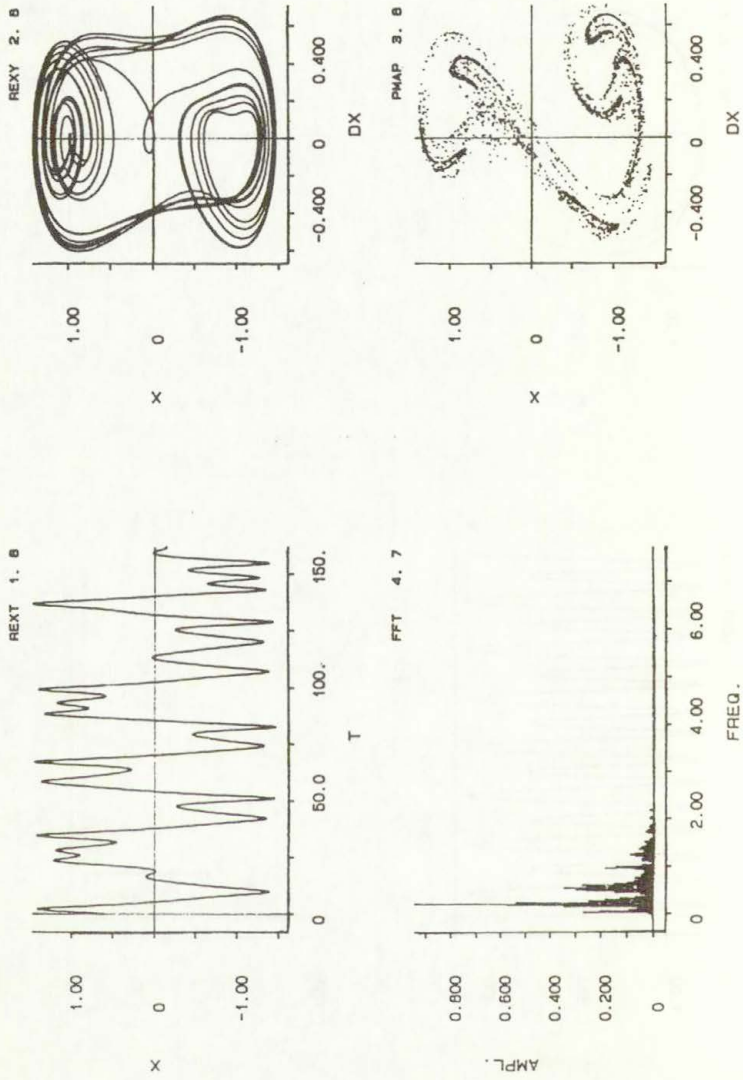Fig. 7c. ω = 0.97.

Fig. 7d. $\omega = 0.93$.

Fig. 7e. ω = 0.79.

Fig. 7f. ω = 0.85.
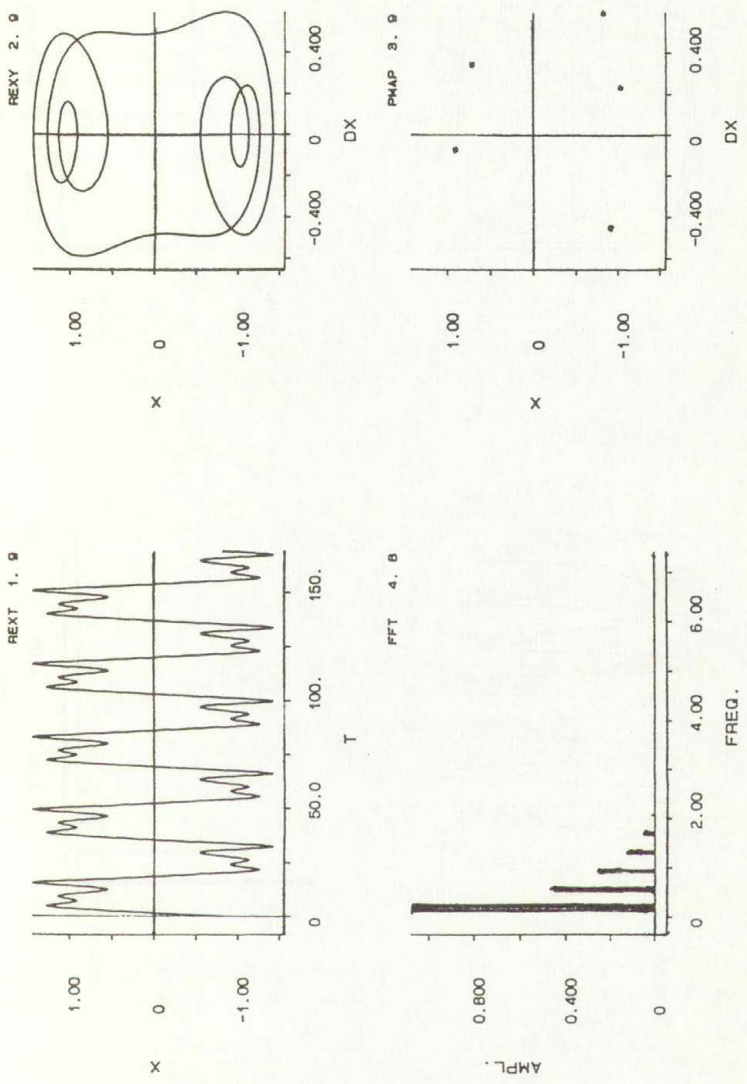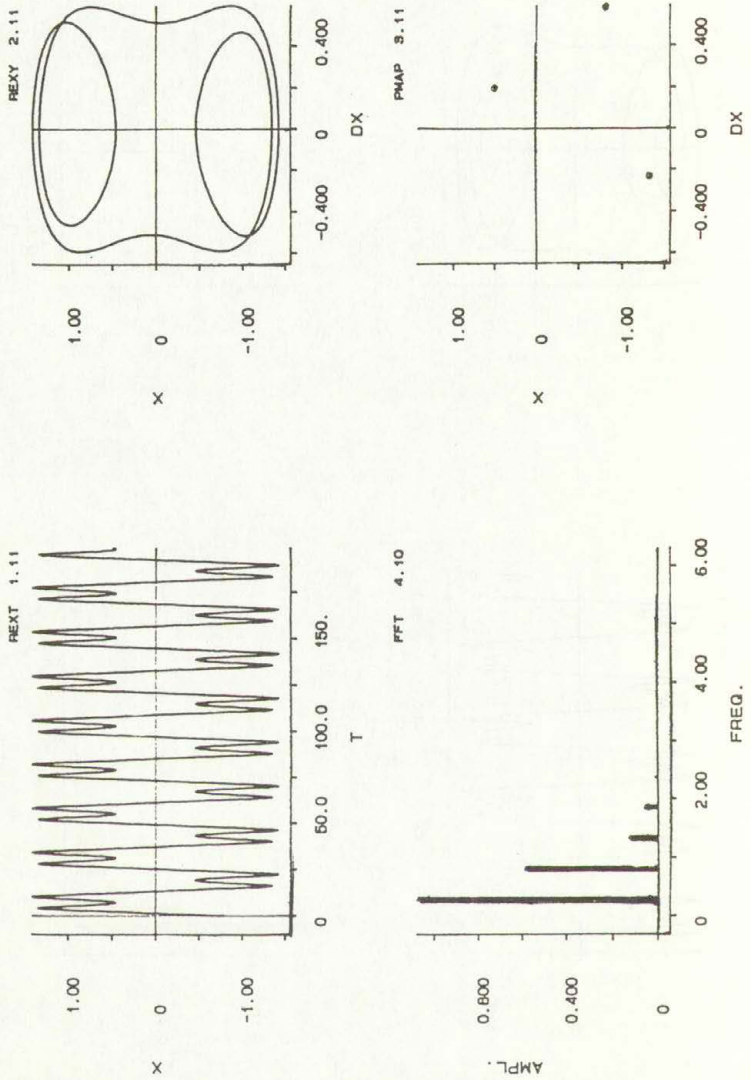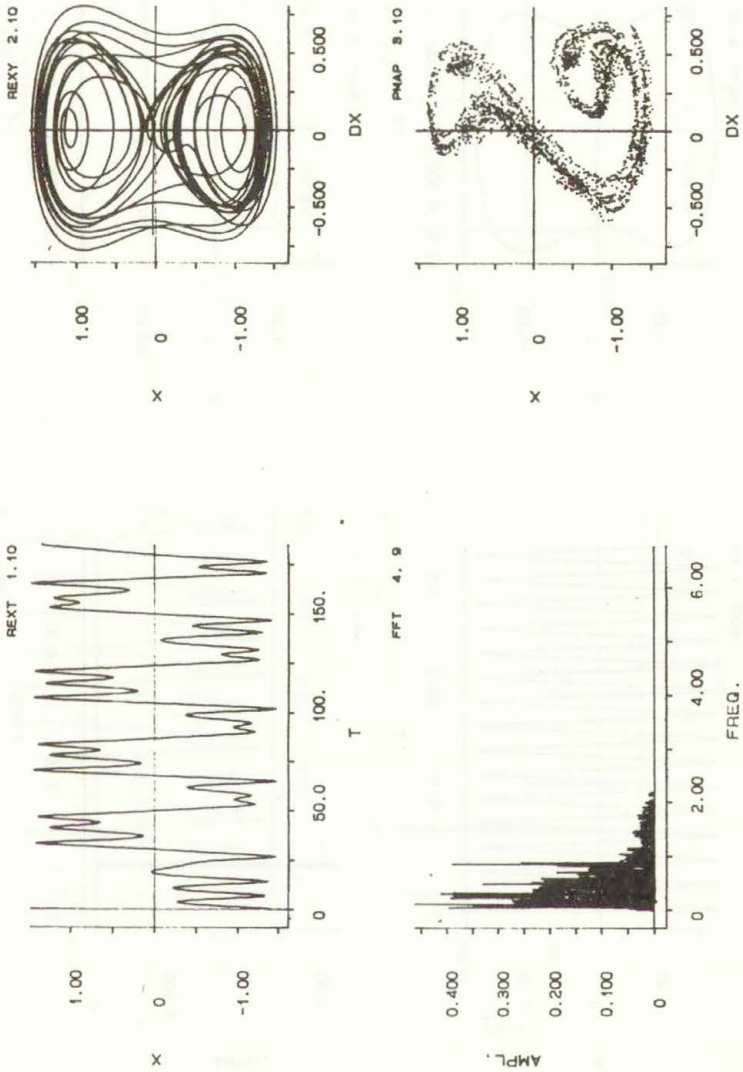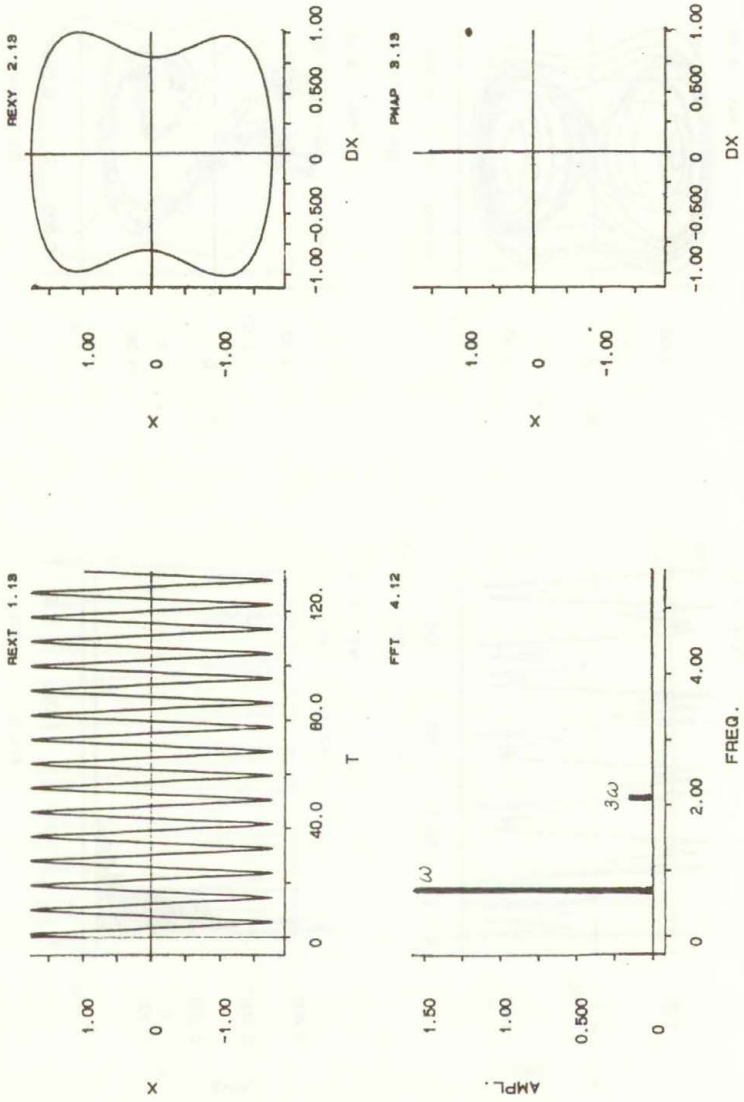
Fig. 7g. ω = 0.7.
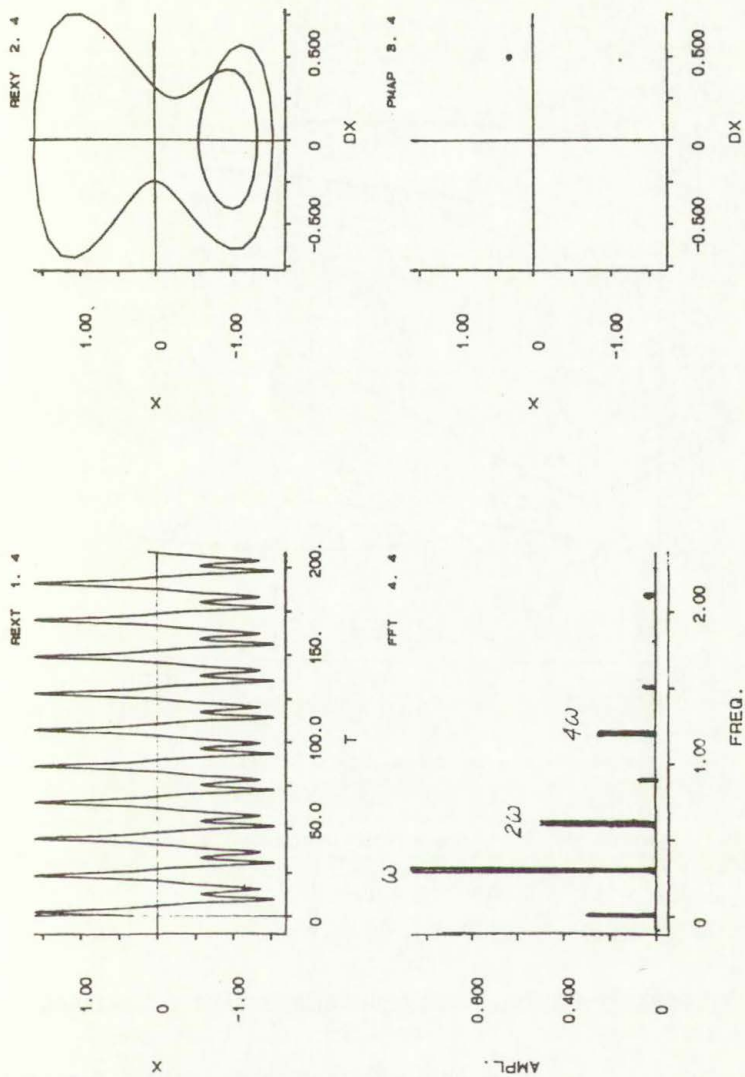
Fig. 8a. Superharmonic resonance of Large Orbit motion:
F = 0.17, ω = 0.30, h = 0.1. Four characteristics of
the response.
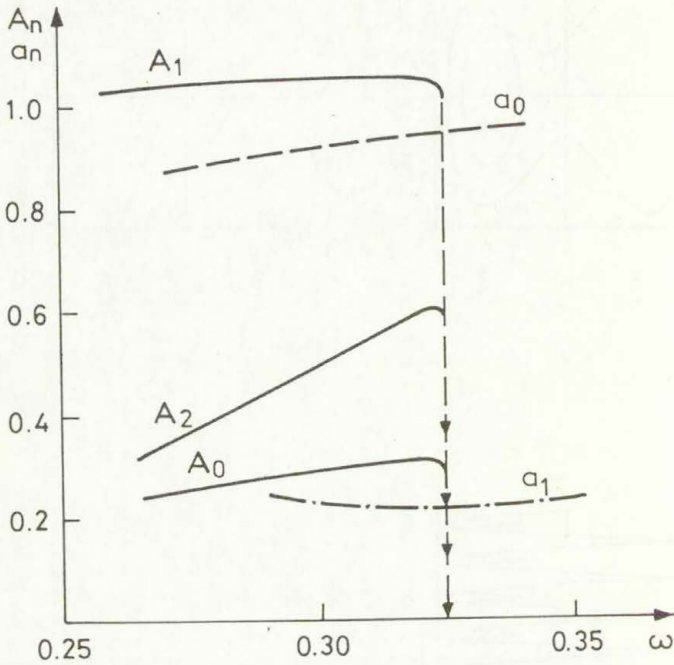
Fig. 8b. Superharmonic resonance of Large Orbit motion:

$F = 0.17$, $\omega = 0.30$, $h = 0.1$.

$A_0$, $A_1$, $A_2$ - resonance curve of L.O.

$a_0$, $a_1$      - resonance curve of S.O.

## 3. LARGE ORBIT T-PERIODIC SOLUTION: APPROXIMATE THEORETICAL ANALYSIS.

In previous section we noticed, that Large Orbit T-periodic motion within a wide range of driving frequency is close to harmonic function of time, with the frequency $\omega$. This makes us

believe, that the first approximate solution and analysis of stability of the solution might give good estimation of the system parameter domain, in which Large Orbit occurs.

With this aim in mind we seek T-periodic solution of eqs. (3) by a perturbation method, the solution which is close to harmonic function of time as:

$$\bar{x}^{(0)} = A_1 \cos (\omega t + \varphi) \; ;$$

We have, therefore, to transform eqs. (1, 3) into the form:

$$(5) \qquad \ddot{\bar{x}} + \omega^2 \bar{x} + \mu f(x, \dot{x}, \omega t) = 0 \; ;$$

To make the transformation possible, we first examine natural oscillation of the system and notice, that the natural frequency, which is imaginary for linearized system, i.e. at $\beta = 0$, becomes real, when the amplitude becomes sufficiently large. Therefore we set $F = h = 0$ and assume harmonic solution as

$$(6) \qquad \bar{x} = A_1 \cos \Omega t \; ;$$

Applying one of approximate techniques, such as: harmonic balance method or equivalent linearization method, we obtain

$$(7) \qquad \Omega^2(A_1) = -\frac{1}{2} + \frac{3}{8}A_1^2 \; ;$$

The natural frequency $\Omega^2(A_1)$ is positive if

$$A^2 > \frac{4}{3} \; ;$$

Now we can write

$$(8) \qquad -\frac{1}{2}\bar{x} + \frac{1}{1}\bar{x}^3 - \Omega^2(A_1) = O(\mu^2) \; ,$$

and consequently we rewrite eqs (5) into:

$$(9) \qquad \ddot{\bar{x}} + \omega^2 \bar{x} + \mu(\bar{h}\dot{\bar{x}} + x\sigma - \Omega^2(A_1)x - \bar{\alpha}\bar{x} + \bar{\beta}\bar{x}^3 - \bar{F} \cos \omega t) = 0$$

where

$$\mu\bar{h} = h \ ; \qquad \mu\sigma = \Omega^2(A_1) - \omega^2 \ , \quad \mu\bar{\alpha} = \frac{1}{2} \ , \quad \mu\bar{\beta} = \frac{1}{2} \ , \quad \mu\bar{F} = F \ .$$

From numerous perturbation techniques, which are available in the literature on the subject (Bogoliubov and Mitropolski [31], Nayfeh [32], Nayfed and Mook [33], Hayashi [34], Szemplińska [35]) the most popular is that called multiple-scale method. It applies a transformation of variables by introducing different time scales:

$$T_0 = t \ , \qquad T_1 = \mu t \ , \quad T_2 = \mu^2 t \ , \quad \ldots \ ,$$

and assumes the solution in the power series of $\mu$ as:

$$(10) \qquad \bar{x}(t,\mu) = \bar{x}_0(T_0,T_1,T_2\ldots) + \mu\bar{x}_1(T_0,T_1,T_2\ldots) + \mu^2\ldots \ ,$$

where the slow scales $T_n$, $n \geq 2$ characterize the modulation in the amplitude and phase caused by nonlinearity, damping and excitation. In terms of the new variable the time derivative are:

$$(11) \qquad \frac{d}{dt} = D_0 + \mu D_1 + \mu^2 D_2 \ \ldots \ ,$$

$$\frac{d^2}{dt^2} = D_0^2 + \mu \ 2D_0D_1 + \mu^2(2D_0D_1 + D^2) + \ldots \ ,$$

where $D_n = \dfrac{\partial}{\partial T_n}$ .

For the sake of clarity we apply an equivalent perturbation technique, the technique which represents the modulation of the amplitude and phase explicitly, not introducing any changes of variables. Therefore we assume the approximate solution of eq. (9) in the following power series of $\mu$,

(12a)    $\bar{x}(\mu,t) = A_1 \cos(\omega t + \varphi) + \mu \bar{x}_1(A_1,\varphi,t) + \mu^2 \ldots$ ,

(12b)    $\dfrac{dA_1}{dt} = \mu D_1(A_1,\varphi) + \mu^2 D_2(A_1,\varphi) + \ldots$ ,

(12c)    $\dfrac{d\varphi}{dt} = \mu E_1(A_1,\varphi) + \mu^2 E_2(A_1,\varphi) + \ldots$ ,

where, in the sought steady state solution, we put:

(13)    $\dfrac{dA_1}{dt} = \dfrac{d\varphi}{dt} = 0$ .

In fact this is the asymptotic method developed first by Bogoliubov and Mitropolski [31] (see also Szemplińska [35]).

Differentiating eqs.12a-c, substituting into eq. (9) and equating coefficients of like power of $\mu$, we obtain

(14)    $\ddot{\bar{x}}_1 + \omega^2 \bar{x}_1 = (2D_1\omega + \bar{h}\omega A_1 + \bar{F} \sin \varphi)\sin \theta + (2E_1 A_1 \omega - \sigma A_1 +$

$+ \bar{F} \cos \varphi) \cos \theta - \dfrac{1}{4}\bar{\beta}A_1^3 \cos 3\theta$ ;

$\theta = \omega t + \varphi$ ;

Elimination of secular terms in $\bar{x}_1(t)$ i.e. equating coefficients of $\cos \theta$ and $\sin \theta$ to zero, yields:

(15)    $2D_1\omega + \bar{h}\omega A_1 + \bar{F} \sin \varphi = 0$ ,

$A_1(2E_1\omega - \sigma) + \bar{F} \cos \varphi = 0$ ;

The steady-state condition (13) is now reduced to the condition

$D_1 = E_1 = 0$ ,

and eq (15) give us the desired amplitude and phase as:

(16)    $A_1 = \dfrac{F}{\sqrt{[\Omega^2(A_1) - \omega^2]^2 + h^2\omega^2}}$ ,    $\text{tg } \varphi = \dfrac{-h\omega}{\Omega^2(A_1) - \omega^2}$ ,

where

$\Omega^2(A_1) = -\dfrac{1}{2} + kA_1^2$ ,    $k = \dfrac{3}{8}$ ;

Next we solve eq (14), (15) to obtain the correction function $\bar{x}_1(t)$:

(17)     $\mu\bar{x}_1(t) = A_3\cos 3(\omega t + \varphi)$ ,

$A_3 = \dfrac{\mu\bar{\beta}A_1^3}{32\omega^2} = \dfrac{A_1^3}{64\omega^2}$ ;

Finally, the refined first approximate solution, which describes Large Orbit motion is:

(18)     $\bar{x}(t) = A_1\cos (\omega t + \varphi) + A_3\cos 3(\omega t + \varphi) = \bar{x}(t + T)$ ,

where $A_1$, $\varphi$, $A_3$ are defined by eq. (16), (17).

To examine stability of the solution we first look at the form of instability, which manifests itself by an exponential growth with time of the harmonic components, which are involved in $\bar{x}(t)$. We do this by adding small disturbances to amplitudes and phases i.e. by considering the disturbed solution as:

(19)     $\tilde{x}(t) = (A_1 + \delta A_1)\cos(\omega t + \varphi + \delta\varphi) +$

$+ (A_3 + \delta A_3)\cos 3(\omega t + \varphi + \delta\varphi)$ ,

$\delta A_3 \equiv \delta A_3(\delta A_1)$ ,

and by making use of eqs. (12b,c), which in the first approximation considered are reduced to:

(20a)     $\dfrac{dA_1}{dt} = \mu D_1(A_1,\varphi)$ ,          $\dfrac{d\varphi}{dt} = \mu E_1(A_1,\varphi)$ ,

where $D_1$, $A_1$ are given by eqs. (15). Adding small disturbances to the steady-state solution (16-18), expanding the right hand side of eqs. (20) into Taylor series and rejecting higher powers of $\delta A_1$, $\delta\varphi$, we obtain linear variational equations with constant coefficients:

(20b)
$$\frac{d\delta A_1}{dt} = \mu \left( \frac{\partial D_1}{\partial A_1} \delta A_1 + \frac{\partial D_1}{\partial \varphi} \delta \varphi \right) ;$$

$$\frac{d\delta \varphi}{dt} = \mu \left( \frac{\partial E_1}{\partial A_1} \delta A_1 + \frac{\partial E_1}{\partial \varphi} \delta \varphi \right)$$

For a particular solution of eqs. (20b):

$\delta A_1 = C_1 e^{\lambda t}$, $\delta \varphi = C_2 e^{\lambda t}$,

the characteristic equation for $\lambda$ is

$\lambda^2 + b\lambda + C = 0$ ,

where $b > 0$ in the dissipative system $(h > 0)$ and

(21)
$$C = \mu^2 \left( \frac{\partial D_1}{\partial A_1} \frac{\partial E_1}{\partial \varphi} - \frac{\partial D_1}{\partial \varphi} \frac{\partial E_1}{\partial A_1} \right) ;$$

From Routh-Hurwitz criterion we learn, that the real values of the roots $\lambda_1$, $\lambda_2$ are positive, i.e. the solution is unstable if

$C < 0$ , $\qquad$ $Re(\lambda_i) > 0$ .

The stability limit is defined by $C = 0$ and the condition is satisfied at those points of the resonance curve $A_1(\omega)$, $\varphi(\omega)$, which have vertical tangent

(22a)
$\qquad$ $C = 0$ , $\qquad$ $\dfrac{d\varphi}{d\omega} = \dfrac{dA_1}{d\omega} = \infty$ ;

$\qquad$ $Re(\lambda_i) = 0$ , $\qquad$ $i = 1$ or $2$ .

Moreover we know, that unstable branches of the resonance curve are those, for which $\dfrac{dA_1}{d\omega}$ and $\omega - \Omega(A_1)$ have the same sign:

(22b)
$\qquad$ $C < 0$ , $Re(\lambda_i) > 0$ , $i = 1$ or $2$

$\qquad$ $\dfrac{dA_1}{d\omega} > 0$ and $\omega - \Omega(A_1) > 0$ $\quad$ or

$\qquad$ $\dfrac{dA_1}{d\omega} < 0$ and $\omega - \Omega(A_1) < 0$

The stability limit parameters can be easily derived by differentiating eqs. (16) with the result

(22c)     $\omega_1^4 - 2\bar{B}\omega_1^2 + \bar{C} = 0$

where

$\bar{B} = 1 + 2kA_1^2 - \dfrac{h^2}{2}$ ,

$\bar{C} = \Omega^4(A_1) + 2kA_1^2\Omega^2(A_1)$ ,

and $\omega_1 \equiv \omega_B$ - the stability limit on the resonant branch of $A_1(\omega)$,

$\omega_1 \equiv \omega_A$ - the stability limit on the nonresonant branch (see Figs. 3, 9-12).

The unstable regions examined by eqs. (19-22c) are referred to as the first order instabilities and an analysis of this type is commonly used in the approximate theory of nonlinear oscillations (e.g. Bogoliubov and Mitropolski [31], Hayashi [34], Nayfeh and Mook [33], Szemplińska [35]). It is worth noticing, that the first order instability occurs in the region of the system parameters where more than one solution for $A_1 \equiv A_1(\omega)$ exists. Therefore the criterion (22b) eliminates some branches of the resonance curves, leaving us with other branches, which seem to be "stable".

To examine other forms of possible instabilities of the periodic solution (18) we should consider other functions for the disturbance $\delta x$, the function, which are not confined to that imposed by eqs. (19). We do this by adding a small disturbance $\delta x$ to $x(t)$:

(23)     $\tilde{x}(t) = \bar{x}(t) + \delta x$ ,

and considering the variational equation for $\delta x(t)$. For small disturbance, terms of order $(\delta x)^n$, $n \geq 2$ are rejected, and the linear variational equation yields:

(24)     $\delta\ddot{x} + h\delta\dot{x} + \dfrac{\partial f}{\partial x}\Big|_{x(t)} \delta x = 0$ ,     $f \equiv -\dfrac{1}{2}x + \dfrac{1}{2}x^3$ ;

Inserting eqs. (18) and expanding the term $\left.\dfrac{\partial f}{\partial x}\right|_{x(t)}$ into Fourier series, we obtain:

(25)
$$\delta\ddot{x} + h\delta\dot{x} + \delta x \,[\lambda_0 + \sum_{n=2,4,6} \lambda_n \cos n\omega t] = 0 \ ,$$

$$\lambda_0 = -\frac{1}{2} + \frac{3}{4}A_1^2 + \frac{3}{4}A_3^2 \ ,$$

$$\lambda_2 = \frac{3}{4}A_1^2 + \frac{3}{2}A_1 A_3 \ ,$$

$$\lambda_4 = \frac{3}{2}A_1 A_3 \ ,$$

$$\lambda_6 = \frac{3}{4}A_3^2 \ ,$$

Introducing new variable $\eta$ by the aid of transformation:

(26a)
$$\delta x = \eta e^{-\frac{h}{2}t} \ ,$$

enables us to reduce eqs. (25) to the Hill's type equation:

(26b)
$$\ddot{\eta} + \eta \,[\lambda_0 - \frac{h^2}{4} + \sum_{n=2,4,6} \lambda_n \cos n\omega t] = 0 \ ;$$

We note, that period of the time dependent coefficient $\displaystyle\sum_{n=2,4,6} \lambda_n \cos n\omega t$ is

(26c)
$$T_1 = \frac{T}{2} \ .$$

Therefore, by virtue of the Floquet theorem, particular solutions of eqs. (25) can be sought as:

(27)
$$\eta(t) = e^{\varepsilon_1 t}\phi(t) \ , \qquad \delta x(t) = e^{\varepsilon t}\phi(t) \ , \qquad \varepsilon = \varepsilon_1 - \frac{h}{2} \ ,$$

where $\varepsilon$ is real and positive in unstable regions and $\phi(t)$ is periodic function of time, with the period $2T_1$, or $T_1$:

(28a)  $\phi_I(t) = \phi_I(t + 2T_1) \equiv \phi_I(t + T)$ ;

(28b)  $\phi_{II}(t) = \phi_{II}(t + T_1) \equiv \phi_{II}(t + \frac{T}{2})$ ;

Functions $\phi_I$, $\phi_{II}(t)$ can be expanded in the Fourier series as (Bolotin [36], Hayashi [34]):

(29a)  $\phi_I(t) = \sum_{n=1,3,5...} b_n \cos n(\omega t + \delta_n)$ , $\omega \approx \dfrac{\sqrt{\lambda_0}}{k}$ , $k = 1,3,5,...$

(29b)  $\phi_{II}(t) = \sum_{n=0,2,4...} b_n \cos (n\omega t + \delta_n)$ , $\omega \approx \dfrac{\sqrt{\lambda_0}}{k}$ , $k = 2,4,...$

The unstable regions emanate from the $\omega$-axis at $\omega = \dfrac{2\sqrt{\lambda_0}}{k}$, where $k$ is an odd integer, (eqs. 28a, 29a), or $k$ is an even integer (eqs. 28b, 29b). They are referred to as odd and even order instabilities, respectively.

Eqs. (28a,b 29a,b) tell us, that none of the instabilities brings a growth of period 2T harmonic components, so that Period Doubling bifurcation does not occur. Type II instability brings, however, another interesting phenomena: it results in a build-up of even order harmonics. This we call Symmetry Breaking instability, the form of instability which is a strong indicator of Symmetry Breaking Bifurcation. Note, that the conclusion which is now drawn from the approximate analysis is in full agreement with general results based on qualitative, topological methods and computer based studies (Hubermann and Crutchfield [37], Raty, von Boem and Isomäki [38], Swift and Wiesenfeld [39], Nayfeh and Sanchez [40]).

To examine the symmetry breaking instability of the symmetric solution (18), we assume two-term solution in eqs. (27, 29b) as:

(30)  $\eta(t) = e^{\varepsilon_1 t} (b_0 + b_{21} \cos 2\omega t + b_{22}\sin 2\omega t)$ ;

Then we insert it into eqs. (25) and apply harmonic balance

method, i.e. we equate constant term, coefficients of cos 2ωt and of sin 2ωt separately to zero. This gives us a set of linear, algebraic, homogeneous equations for $b_0$, $b_{21}$, $b_{22}$.

Equating to zero the characteristic determinant, we obtain:

$$(31) \quad \Delta(\varepsilon_1^2) = \begin{vmatrix} \lambda_0 + \varepsilon_1^2 - \dfrac{h^2}{4} \, , & \dfrac{\lambda_2}{2} & , & 0 \\[2ex] \lambda_2 & , -4\omega^2 + \lambda_0 - \dfrac{h^2}{4} + \varepsilon_1^2 + \dfrac{\lambda_4}{2} \, , & 4\omega\varepsilon_1 \\[2ex] 0 & , \qquad -4\omega\varepsilon_1 & , -4\omega^2 + \lambda_0 - \dfrac{h^2}{4} + \varepsilon_1^2 - \dfrac{\lambda_4}{2} \end{vmatrix} = 0,$$

At the stability limit, where $\varepsilon_1^2 - \dfrac{h^2}{4} = 0$, the above determinant is reduced to:

$$(32a) \quad \Delta(h^2) = \begin{vmatrix} \lambda_0 \, , & \dfrac{\lambda_2}{2} & , & 0 \\[2ex] \lambda_2 \, , & -4\omega^2 + \lambda_0 + \dfrac{\lambda_4}{2} \, , & 4\omega h \\[2ex] 0 \, , & -4\omega h & , \; -4\omega^2 + \lambda_0 - \dfrac{\lambda_4}{2} \end{vmatrix} = 0 \, ,$$

This result is a quadratic polynomial for $\omega^2$:

$$(32b) \quad \omega_{SB}^4 - 2B\omega_{SB}^2 + C = 0 \, , \qquad B \equiv B(A_1) \, , \qquad C \equiv C(A_1) \, ;$$

and gives us the desired relationship between $\omega$ and the amplitude $A_1$ to be satisfied at the Symmetry Breaking instability limit:

$$(32c) \quad \omega_{SB} \equiv \omega_{SB}(A_1) \, ;$$

To make sure, which region in $A_1 - \omega$ plane corresponds to unstable solution, we expand the determinant (31) into power

series in the neighborhood of $\varepsilon_1^2 - \frac{h^2}{4} = 0$. For small values of $\varepsilon_1^2 - \frac{h^2}{4}$ we reject higher power terms and obtain:

(33)  $\Delta(\varepsilon_1^2) = \Delta(h^2) + \left.\frac{\partial\Delta}{\partial\varepsilon_1^2}\right|_{\varepsilon_1^2 - \frac{h^2}{4} = 0} (\varepsilon_1^2 - \frac{h^2}{4}) = 0$ ;

Noticing that $\frac{\partial\Delta}{\partial\varepsilon_1^2} > 0$ in the whole range of amplitudes considered, we conclude that in the unstable region:

(34)  $\varepsilon_1^2 - \frac{h^2}{4} > 0$ ,

$\Delta(h^2) < 0$ .

We conclude, therefore, that the resonant branch of $A_1 = A_1(\omega)$, which seems to be stable in the sense of criterion (22b), is unstable in the sense of Symmetry Breaking instability criterion (34) at $\omega < \omega_{SB}$, (see Fig. 9). To determine the Symmetry Breaking stability limit in the $F - \omega$ plane, we calculate the forcing parameter F by the aid of eq. (16)

(35)  $F_{SB} = \sqrt{(\Omega^2(A_1) - \omega_{SB}^2)^2 + h^2\omega_{SB}^2}$

Fig. 10 depicts both stability limits in the $F - \omega$ plane: the first order stability limit, which coincides with p. B in Fig. 9 and the Symmetry Breaking stability limit defined by eqs. 32b. The computer simulations results presented alresdy in Fig. 5 are shown again, for comparison. We see, that the theoretical $\omega_B(F)$ values are very close to the true boundary of existence of Large Orbit motion. We notice also that the theoretical Symmetry Breaking stability limit $\omega_{SB}$ overestimates the values of driving frequency, for which symmetry breaking instability really occurs. This is, however, due not only to low order approximation used in the theoretical solution, but also to the fact, that in the computer based studies we determine the values
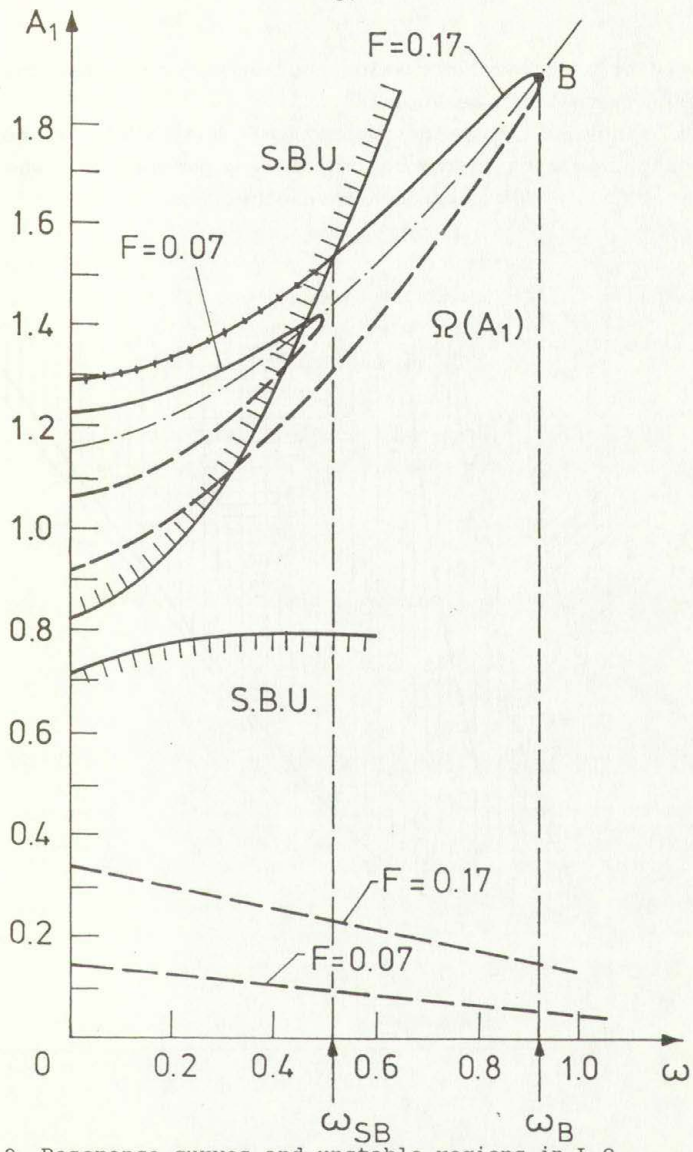
Fig. 9. Resonance curves and unstable regions in L.O.
approximate solution:
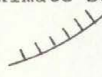
Symmetry Breaking instability

of driving frequency, for which the even order harmonics are
that large that can be detected.

It is obvious, that the theoretical analysis can not give
reasonable results in the region of F, $\omega$ parameters, where the
two stability limits approach each other.



Fig. 10. Regions of L.O. attractor: computer simulation and
theoretical stability limits: h= 0.1.

## 4. SMALL ORBIT MOTION: APPROXIMATE THEORETICAL ANALYSIS.

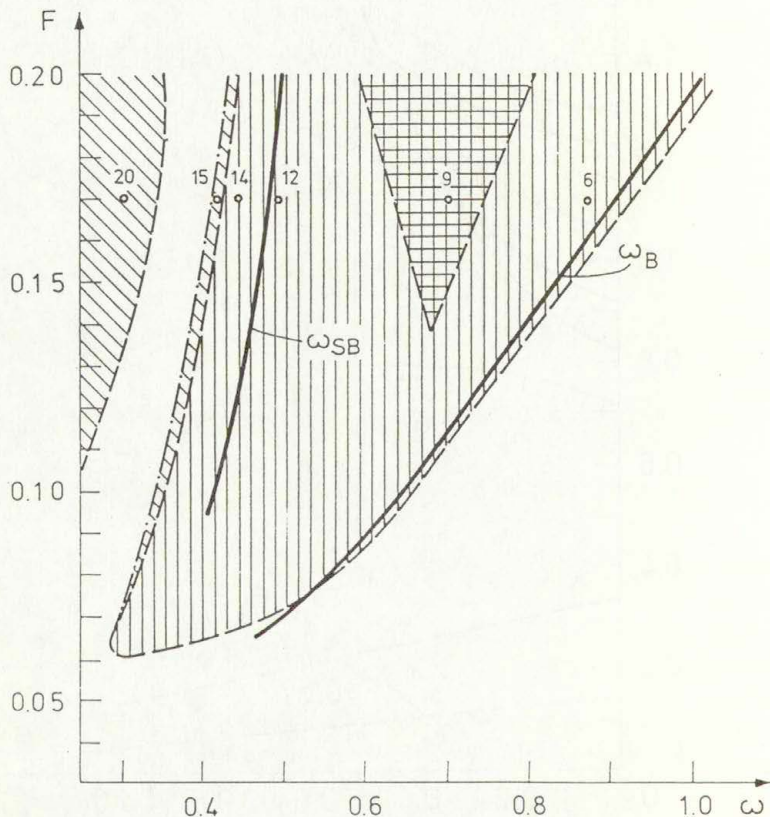Computer simulations, presented in section 2, revealed, that the Small Orbit motion in the neighborhood of the principal resonance is very close to harmonic function of time with the frequency $\omega$, even at high values of the forcing parameter, at $F > F_2$. This is true for the values of the driving frequency which are outside the zone defined by $\omega_A$ and $\omega_{PDB}$ (see Fig. 3c), when $\omega_A$ is the cycle fold bifurcation point, and $\omega_{PDB}$ - denotes the first period doubling bifurcation.

Therefore, we consider T-periodic solution of eq. (4), the solution which is close to:

(36)     $x^{(0)}(t) = a_1 \cos (\omega t + \varphi)$ ,

and we seek an answer to the question, whether approximate analysis of various forms of instability of the solution can be useful in predicting the true $\omega_A$ and $\omega_{PDB}$ values, and thus whether it enables us to construct approximate criteria for steady-state cross-well chaotic motion.

To apply perturbation methods we transform eqs. (4) into the form:

(37)     $\ddot{x} + \omega^2 x + \mu \bar{\alpha}_2 x^2 + \mu^2 [\bar{h}x + \bar{\alpha}_3 x^3 + \sigma x - \bar{F} \cos \omega t] = 0$ ,

where
$$\mu \bar{\alpha}_2 \equiv \frac{3}{2} , \qquad \mu^2 \bar{\alpha}_3 = \frac{1}{2} , \qquad \mu^2 \bar{h} = h , \qquad \sigma \mu^2 = 1 - \omega^2 ,$$
$$\mu^2 \bar{F} = F , \qquad \mu - \text{small parameter.}$$

Note, that we put the quadratic term to be of order $\mu^1$, with all other terms to be proportional to $\mu^2$, and that the assumption is not related to the magnitudes of respective coefficients. The relation between $x^2$ and $x^3$ terms comes from a rescaling properties. Setting damping, detuning parameter and forcing term of order that of $x^3$ is motivated by the fact, that

perturbation methods need higher approximation to capture effects of quadratic term. The assumed form of eq. (32) gives us, therefore, good opportunity to account properly for the quadratic term and to obtain the second approximate solution in as simple form as possible.

Next we apply the perturbation technique,which was used in section 3, and assume solution of eq. (37) in the form:

(38a)  $x(t) = a_1 \cos(\omega t + \varphi) + \mu x_1(a_1, \varphi, t) + \mu^2 \ldots$

(38b)  $\dfrac{da_1}{dt} = \mu D_1(a_1, \varphi) + \mu^2 D_2(a_1, \varphi) + \mu^3 \ldots$

(38c)  $\dfrac{d\varphi}{dt} = \mu E_1(a_1, \varphi) + \mu^2 E_2(a_1, \varphi) + \mu^3 \ldots$

The terms of order $\mu^1$ give us:

(39)  $x_1 + \omega^2 x_1 = 2D_1 \omega \sin \theta + 2E_1 \omega\, a_1 \cos \theta - \dfrac{1}{2}\bar{\alpha}_2 a_1^2 - \dfrac{1}{2}\bar{\alpha}_2 a_1^2 \cos 2\theta$ ;

$\theta = \omega t + \varphi$ .

Elimination of secular terms yields:

(40)  $D_1 = E_1 = 0$ ,

and the correction function $x_1(t)$ is

$\mu x_1(t) = a_0 + a_{12} \cos 2\theta$ ,

$a_0 = -\dfrac{1}{2}\bar{\alpha}_2 a_1^2 \mu^2$ ;   $a_{12} = \dfrac{1}{6}\bar{\alpha}_2 a_1^2 \mu^2$ ;

Terms of order $\mu^2$ and eq. (40) yield:

(41)  $\ddot{x}_2 + \omega_2^2 x_2 = (2\omega D_2 + \bar{h} a_1 \omega + \bar{F} \sin \varphi)\sin \theta + [2E_2 a_1 \omega - \dfrac{3}{4}\bar{\alpha}_3 a_1^3$

$- \sigma a_1 + \bar{F} \cos \varphi]\cos \theta - 2\bar{\alpha}_2 a_1 x_1(t) \cos \theta - \dfrac{1}{4}\bar{\alpha}_3 a_1^3 \cos 3\theta$ ;

Elimination of secular terms and the steady-state condition

(42)     $\dfrac{da_1}{dt} = \mu D_1 + \mu^2 D_2 = 0$ ,

$\dfrac{d\varphi}{dt} = \mu E_1 + \mu^2 E_2 = 0$ ,

results in the amplitude and phase solution as:

(43)     $a_1 = \dfrac{F}{\sqrt{(\Omega^2(a_1) - \omega^2)^2 + h^2\omega^2}}$ ,     $tg\ \varphi = \dfrac{-h\omega}{\Omega^2(a_1) - \omega^2}$

where

$\Omega^2(a_1) = 1 - ka_1^2$ ,     $k = \dfrac{5}{6}\mu\bar{\alpha}_2^2 - \dfrac{3}{4}\mu^2\bar{\alpha}_3 = \dfrac{3}{2}$ ;

Finally the second approximate solution for Small Orbit motion close to the principal resonance, $\omega \approx 1$ is

(44)     $x(t) = a_1\cos(\omega t + \varphi) + a_0 + a_2\cos 2(\omega t + \varphi)$ ;

$a_0 = -\dfrac{3}{4}a_1^2$ ,          $a_{12} = \dfrac{1}{4}a_1^2$

and $a_1$, $\varphi$ are given by eqs. (43).

The natural frequency $\Omega(a_1)$ is decreasing with the amplitude, and consequently the resonance curves $a_1 = a_1(\omega)$ are bent to the left (see Fig. 11). They preserve the classic shape and possess the peak amplitude with the point B for which $\dfrac{da_1}{d\omega} = \infty$ unless $F > F_1$. The theoretical limit value of the forcing parameter for point B to exist, at low damping, is:

(45)          $F_1 \approx \dfrac{1}{\sqrt{4k}}$

For $F > F_1$ the resonance curve $a_1 \equiv a_1(\omega)$ look like those for undamped system.

Therefore the first order stability limits, defined by criterion (22c) exist on the nonresonant branch only (point A), and the whole resonant branch seems to be "stable" in the sense of criterion (22b). To examine other forms of instability of the

T-periodic solution (44) we turn to Hill's type variational equation (24), which yields:
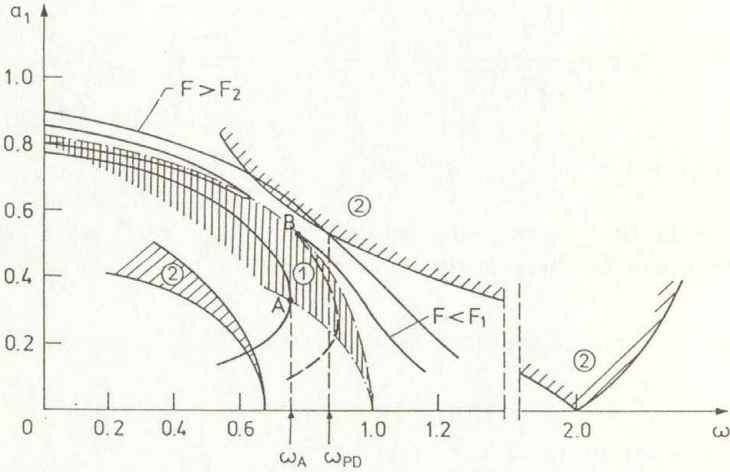


Fig. 11. Resonance curves and two types of unstable regions of S.O. solution: ① - first order instability ② - Period Doubling instability.

(46)    $\delta \ddot{x} + h\delta \dot{x} + \delta x[\lambda_0 + \sum_{n=1}^{4} \lambda_n \cos n\omega t] = 0$ ,

$\lambda_0 = 1 - \frac{3}{2}a_1^2 + \frac{57}{64}a_1^4$ ,

$\lambda_1 = 3a_1 - \frac{15}{8}a_1^3$ ,

$\lambda_2 = \frac{3}{2}a_1^2 - \frac{9}{16}a_1^4$ ,

$\lambda_3 = \frac{3}{8}a_1^3$ ,

$\lambda_4 = \frac{3}{64}a_1^4$ ;

Note, that period of time-dependent term $T_1$ equals to the period of x(t):

(47) $\qquad T_1 = T \; ;$

Therefore, the two types of instability defined by eqs. (28 a,b, 29 a,b) now are:

$$\delta x(t) = e^{(\varepsilon_1 - \frac{h}{2})t} \phi(t)$$

(48a) $\qquad \phi_I(t) = \phi_I(t + 2T) = \sum_{n=1,3,5...} b_n \cos (\frac{n\omega}{2}t + \delta_n) \cdot ,$

$$\omega \approx \frac{2\sqrt{\lambda_0}}{k} , \qquad\qquad k = 1, 3, 5, \ldots$$

(48b) $\qquad \phi_{II}(t) = \phi_{II}(t + T) = \sum_{n=0,2,4...} b_n \cos (\frac{n\omega}{2}t + \delta_n) ,$

$$\omega \approx \frac{2\sqrt{\lambda_0}}{k} , \qquad\qquad k = 2, 4, 6, \ldots$$

We notice immediately that the odd type instability given by eqs. (48a) brings a growth with time of the harmonic components, which have period 2T. This is, therefore, Period Doubling instability, which leads to Period Doubling Bifurcations.

To examine the instability, we assume two term solution for $\delta x(t)$ as:

(49) $\qquad \delta x(t) = e^{(\varepsilon_1 - \frac{h}{2})t} \sum_{n=1,3,5...} (b_{nc} \cos \frac{n\omega}{2}t + b_{ns} \sin \frac{n\omega}{2}t)$

and we follow the procedure, which was outlined in sec. 3. Finally we arrive at the fourth order determinant and the fourth order polynomial for the desired $\omega_{PD}$:

(50) $\qquad \Delta_4(a_1, \omega, h) = 0$

$\qquad \omega_{PD}^8 + b_6 \omega_{PD}^6 + b_4 \omega_{PD}^4 + b_2 \omega_{PD}^2 + b_0 = 0 \; ;$

If we neglect damping in the variational equation (46) we can set $b_{ns} = 0$, $h = 1,2$. in the solution (49) and thus to reduce eqs. (50) to the quadratic equation for $\omega_{PD}$. The simplification appears to give surprisingly good results even at damping coefficient that high as 0.2 (see Szemplińska, Plaut and Hsieh [15]). This can be explained by the fact that boundaries of unstable regions are strongly affected by damping at low values of parametric excitation term ($\lambda_1$, $\lambda_2$... in eqs. 46). We are, however, exploring regions of high magnitudes of the amplitude $a_1$, and so of the coefficient $\lambda_n$, the region where the effect of damping is negligible (Hayashi [34]).

Setting $h = 0$ in eqs. (50), we obtain:

(51)     $\Delta_2 = \omega_{PD}^4 - 2B\omega_{PD}^2 + C = 0$ ,

where:

$$B = \frac{20}{9}\lambda_0 + \lambda_1 + \frac{1}{9}\lambda_3 \ ,$$

$$C = \frac{16}{9} \ [ \ (\lambda_0 + \frac{\lambda_1}{2})(\lambda_0 + \frac{\lambda_3}{2}) - \frac{1}{4}(\lambda_1 + \lambda_2)^2 ] \ ,$$

and $\lambda_1 = \lambda_L(a_1)$ are given by eqs. (46).

In the unstable region the determinant is negative: ·

(52)          $\Delta_2 < 0$    if $\varepsilon_1^2 - \frac{h^2}{4} > 0$ .

The resonance curves $a_1 = a_1(\omega)$ and the two types of unstable regions: the first order instability defined by eqs. (22b) and the Period Doubling unstable regions given by eqs. (51, 52) are depicted in Fig. 11. The two-term solution (49) gives us two Period Doubling unstable regions: one which emanates from the $\omega$-axis at $\omega = 2$, and the other – at $\omega = \frac{2}{3}$ . At low amplitudes they correspond to the 1/2 subharmonic resonance and 3/2 supersubharmonic resonance, respectively. We see, however, that the Period Doubling instability visits also the principal resonance region and the stability boundary crosses the resonant branch of $a_1 = a_1(\omega)$, if the forcing parameter F exceeds certain

critical value, the value denoted as $F_2$. For $F > F_2$ the resonant branch of $a_1(\omega)$ loses stability by Period Doubling at $\omega = \omega_{PD}$, while the nonresonant branch has lost its stability at the point with vertical tangent - at $\omega_A$. We may conclude, therefore, that within the range

$$\omega_A < \omega < \omega_{PD}$$

the T-periodic solution is unstable, and that "strange phenomena" can be expected.

We could continue to examine stability of the resonant branch by considering 2T periodic solution and again studying a corresponding variational equation. This would have led us to the second bifurcation, and further to the cascade of Period Doublings. The computer based studies, which revealed that the cascade of bifurcations occurs in a very narrow frequency band $\Delta\omega$ (see Fig.3c, 5) allow us to confine our theoretical analysis to the first bifurcation.

The theoretical stability boundary defined by the frequency $\omega_A$ and $\omega_{PD}$ are plotted in $F - \omega$ plane and compared to the computer simulation results (Fig. 12). We see, that the crude approximation analysis, which provides us with simple, close form algebraic formulae for the two stability limits, gives surprisingly good estimation of the system parameter critical values, the values for which cross-well chaos really occurs.


5. CONCLUDING REMARKS

The computer based studies show, that the twin-well potential oscillator exhibits a great of variety of different steady state motions. Highly regular periodic and complex chaotic attractors are very close to each other in the system parameter domain, and alternate with a change of one parameter. The survey of steady states at fixed damping and fixed forcing allow us to notice, that large amplitude motion can be highly regular, or even close to harmonic function of time, while a smaller amplitude motion appears to be very complex, chaotic. The observation seems to blur a distinction between weak and strong nonlinearity effects.

Computer simulations bring an observation, that the lower frequency boundary of cross-well chaotic motion is related to jump phenomenon, and that upper boundary is separated from T-periodic regular Small Orbit by a very narrow frequency band .
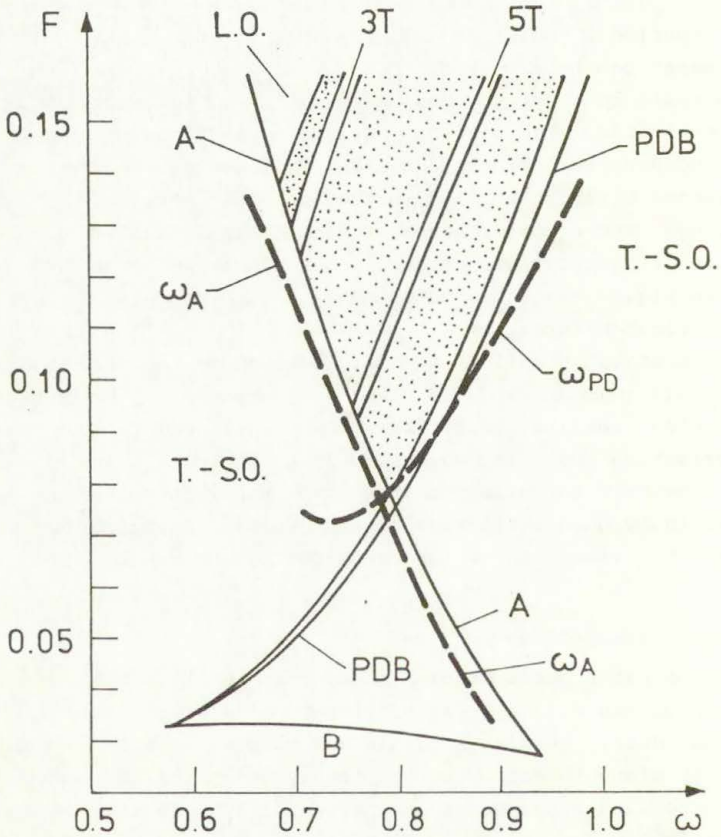


Fig. 12. Regions of S.O. attractor: computer simulations and theoretical stability limit,
▨ - cross-well chaos.

This brings us to the result, that the crude theoretical analysis, the analysis which has its roots in the classic approximate theory of nonlinear oscillations, can give us simple, close form approximate criteria for cross-well chaos.

Also, high regularity of Large Orbit motion enables us to use a low order approximate solution and to obtain good estimation of the system parameter values, where this type of steady state occurs.

## 6. REFERENCES

1. MAHAFFEY R.A. Anharmonic oscillator description of plasma oscillations, Phys. Fluids 19, 1387-1391, (1976).

2. MOON F.C, Experiments on chaotic motion of a forced nonlinear oscillator - strange attractors, ASME J. Appl. Mech., v.47, 638-644, (1980).

3. MOON F.C. and LI C.X., Fractal Basin Boundaries and Homoclinic Orbits for Periodic Motion in a Two-well Potential. Physical Rev. Letters, 55, 1439-1444, (1985).

4. ARECCHI F.T. and CALIFANO A., Low-frequency hopping phenomena in a nonlinear system with many attractors, Physics Letters v. 101A No.9, 443-446, (1984).

5. GREBOGI C., OTT E., and YORKE J.A. Crisis, sudden changes in chaotic attractors, and transient chaos, Physica 7D, 181-200, (1983).

6. GUCKENHEIMER J. and HOLMES P. Nonlinear Oscillations, Dynamical Systems, and Bifurcations of Vector Fields, Springer-Verlag, New York. (1983).

7. HOLMES P.,A nonlinear oscillator with a strange attractor, Phil.Trans. of the Royal Soc. Ser.A, v.292, No.1394, 419-448, (1979).

8. HOLMES P.J. and MOON F,C. Strange Attractors and Chaos in Nonlinear Mechanics, J. of Applied Mechanics 50,1021-1032, (1983).

9. MCDONALD S.W., GREBOGI C, OTT E. and YORKE J.A., Fractal basin boundaries, Physica D, 17, 125-153, (1985).

10. MOON F.C. and LI C.X., The fractal dimension of the two-well potential strange attractor, Physica D, 99-108, (1985).

11. PEZESHKI Ch. and DOWELL E.H., On chaos and fractal behavior in a generalized Duffing's system, Physica D 32, 14-209, (1988).

12. PEZESHKI Ch. and DOWELL E.H., Generation and analysis of Lapunov exponents for the buckled beam. Int. J. Non-Linear Mech, 24, 2, 79-97, (1989).

13. SZEMPLIŃSKA-STUPNICKA W., JOOS G. and MOON F.C., Chaotic Motion in Nonlinear Dynamical Systems, Springer-Verlag, Wien. (1988).

14. SZEMPLIŃSKA-STUPNICKA W., The refined approximate criterion for chaos in a two-state mechanical oscillator, Ing. Archiv 58, 354-366, (1988).

15. SZEMPLIŃSKA-STUPNICKA W., PLAUT R.H and HSIEH J.C., Period doubling and chaos in unsymmstric structures under parametric excitation, J. Applied Mech., 56, 947-952, (1989).

16. TANG D.M. and DOWELL E.H., On the Treshold Force for Chaotic Motions for a Forced Buckled Beam, J. Applied Mech, 55, 190-196, (1988).

17. UEDA Y., YOSHIDA S., STEWART H.B. and THOMPSON J.M.T., Basin explosions and escape phenomena in the twin-well Duffing oscillator: compound global bifurcations organizing behavior, Phil. Trans. R. Soc. London A 332, 169-186, (1990).

18. DOWELL E.H. and PEZESHKI C. , On necessary and sufficient conditions for chaos to occur in Duffing's equation: an heuristic approach; Journal of Sound and Vibration 121(2), 195-200, (1988).

19. DOWELL E.H, Chaotic oscillations in mechanical systems, Computational Mechanics, 199-216, (1988).

20. SZEMPLIŃSKA-STUPNICKA W., The approximate analytical methods in the study of transition to chaotic motion in nonlinear oscillators, Engineering Applications of Dynamics of Chaos, Springer Verlag Wien, 225-278, (1991).

21. SZEMPLIŃSKA-STUPNICKA W, and RUDOWSKI J., Local methods in predicting an occurrence of chaos in the two-well potential system: superharmonic frequency region. J. Sound and Vibration, 151(2), 57-72, (1992).

22. MOON F.C., Chaotic Vibrations, J. Wiley&Sons, New York. (1987).

23. TAKIMOTO N, and YAMASHIDA H., The variational approach to the theory of subharmonic bifurcations, Physica 26 D, 251-276, (1987).

24. VIRGIN L.N., On the harmonic response of an oscillator with unsymmetric restoring force, J. Sound and Vibration, 126 (1), 157-166, (1988).

25. FEIGENBAUM M.J., Quantitative universality for class of nonlinear transformations, J. Stat. Phys. v.19, No.1, 25-52, (1978).

26. THOMPSON J.M.T. and STEWART H.B., Nonlinear Dynamics and Chaos, J.Wiley&Sons, New York, (1986).

27. THOMPSON J.M.T., Chaotic phenomena triggering the escape from a potential well, Proc. R. Soc. London, A 421, 195-225, (1989).

28. THOMPSON J.M.T., Loss of engineering integrity due to the erosion of absolute and transient basin boundaries, Nonlinear Dynamics in Engineering Systems, ed. Schiehlen, Springer-Verlag, Berlin, 313-320, (1989).

29. UEDA Y., Explosions of strange attractors exhibited by Duffing's equation, Annals of N.Y. Academy of Sc., 357, 422-434, (1980).

30. UEDA Y., Steady motions exhibited by Duffing's equation: a picture book of regular and chaotic motions. New Approaches to Non-Linear Problems in Dynamics, SIAM, Philadelphia, 311-322, (1980).

31. BOGOLIUBOV N.N. and MITROPOLSKI Y.A. Asymptotic Methods in the Theory of Nonlilnear Oscillations, Gordon and Breach Science Publishers, New York (1961), (in Russian - 4-th edition, Nauka, Moskva 1974).

32. NAYFEH A.H., Perturbation Methods, J. Wiley, New York, (1973).

33. NAYFEH A.H. and MOOK D.T., Nonlinear Oscillations, J. Wiley, New York. (1979).

34. HAYASHI Ch., Nonlinear Oscilations in Physical Systems, Princeton University Press, Princeton N. J. (1985).

35. SZEMPLIŃSKA-STUPNICKA W., The Behavior of Non-linear Vibrating Systems, Kluwer Academic Publishers, (1990).

36. BOLOTIN V.V., Dynamic Stability of Elastic Systems, Holden-Day, San Francisco (1964).

37. HUBERMAN B.A. and CRUTCHFIELD J.P, Chaotic States of Anharmonic System in Periodic Fields, Physical Review Letters v.43, 1743-1747, (1979).

38. RATY R, J. VON BOEM and ISOMÄKI H.M., Absence of inversion-symmetric limit cycles of even periods and the chaotic motion of Duffing's oscillator, Physics Lett. 103A,289-291, (1984).

39. SWIFT J. and WIESENFELD K, Suppression of period doubling in symmetric systems, Phys.Rev.Lett. 52, 705-710, (1984).

40. NAYFEH A.H. and SANCHEZ N.E, Bifurcations in forced softening Duffing oscillator, Int. J. Non-Linear Mech. 24, 483-497, (1989).